THE ASTROPHYSICAL JOURNAL, 461:920–926, 1996 April 20

ON THE VISCOSITY-DRIVEN SECULAR INSTABILITY IN ROTATING NEUTRON STARS

DAVID SKINNER AND LEE LINDBLOM
Department of Physics, Montana State University, Bozeman, MT 59717
Received 1995 September 20; accepted 1995 October 30

ABSTRACT

Rapidly rotating stars may be subject to a secular instability driven by viscosity. The oscillation modes that are susceptible to this instability are studied here in models of rigidly rotating neutron stars based on the polytropic and on several more realistic equations of state. For the polytropic models we confirm the classical result: that sufficiently rapidly rotating stars with adiabatic index $\gamma > 2.237$ suffer from the viscous instability, while those with $\gamma < 2.237$ do not. For the more realistic models we find no viscous instability in the 1.4 $M_\odot$ models from any equation of state. In sufficiently massive and rapidly rotating models, however, we do find the viscous instability in stars constructed from *some* of the realistic equations of state.

Subject headings: instabilities — stars: interiors — stars: neutron — stars: oscillations — stars: rotation

1. INTRODUCTION

The angular velocity is the most frequently and accurately observed property of neutron stars. It is interesting, therefore, to study the physical mechanisms that might limit the rotation rates of these stars. Understanding these mechanisms would make it possible to make quantitative predictions of the range of angular velocities in neutron stars and these predictions could then be compared with the observations. The possible equilibrium configurations of rotating stars have only a limited range of angular velocities. If a star rotates faster than the angular velocity of a particle in orbit at its surface, then the stellar material on the surface would be ejected. This orbital or "Keplerian" angular velocity $\Omega_{\rm Kep}$ is, therefore, an absolute upper bound on the physically allowed rotation rate for any star. The possible equilibrium states of neutron stars have been studied extensively and this fundamental limit on the angular velocity is now well understood (see, e.g., Friedman, Ipser, & Parker 1989; Lattimer et al. 1990; Cook, Shapiro, & Teukolsky 1994). This effect limits the possible angular velocities to which a nonrotating star of mass M and radius R may be spun up: $\Omega^2 \lesssim GM/3R^3$, where G is Newton's gravitation constant. This expression for the limit is quite accurate ($\pm 5\%$) for a wide range of equations of state of neutron star matter (see Lindblom 1987 and, for a similar limit, Haensel, Salgado, & Bonazzola 1995).

Instabilities may prevent some equilibrium states from being realized physically and so limit further the allowed angular velocities of rotating stars. The secular instability driven by gravitational radiation is one such instability. On its own, gravitational radiation would make some mode in every rotating star unstable (Chandrasekhar 1970; Friedman & Schutz 1977; Friedman 1978). This instability slows the rotation of the star by radiating away its excess angular momentum to infinity in the form of gravitational radiation. Viscosity suppresses this instability in sufficiently slowly rotating stars (Lindblom & Detweiler 1977; Lindblom & Hiscock 1983) and could suppress the instability in all stars if the viscosity of the stellar matter were large enough. Internal dissipation within neutron star matter is in fact quite large, and it suppresses the gravitational radiation secular instability in neutron stars cooler than the superfluid transition temperature $T \lesssim 10^9$ K (Lindblom & Mendell 1995) or hotter than $T \gtrsim 10^{10}$ K (Ipser & Lindblom 1991; Lindblom 1995). Thus, the gravitational radiation secular instability may only influence the rotation rates of neutron stars during their adolescence, as their temperatures cool through the range $10^9 \lesssim T \lesssim 10^{10}$ K. During this phase the gravitational radiation instability can limit the angular velocities to values that are only slightly below the Keplerian value: $\Omega \lesssim 0.9\Omega_{\rm Kep}$ (see, e.g., Lindblom 1995).

In this paper we explore the effect of a different secular instability, the one driven by viscous forces, on the rotation rates of neutron stars. The viscosity-driven secular instability has been known for over a century (Thompson & Tait 1883), and its properties have been investigated from time to time since its discovery (see, e.g., Roberts & Stewartson 1963; James 1964; Lindblom 1987). This instability lowers the rotational kinetic energy of an afflicted star by converting this energy into heat. The earlier investigations of this instability reveal that the viscosity-driven secular instability is not generic (unlike its gravitational radiation counterpart): in sufficiently slowly rotating stars no mode is driven unstable by the viscous forces. Further, the viscosity-driven secular instability is completely absent unless the star is composed of material with a sufficiently "stiff" equation of state (James 1964). In this paper we explore the extent to which this instability might play a role in real neutron stars. We investigate in our more realistic models the particular modes that are known to suffer from the viscosity-driven secular instability in the idealized cases studied previously. We confirm the finding of James (1964) that the viscosity-driven secular instability can occur in polytropic stellar models only if the equation of state is sufficiently stiff, i.e., if the adiabatic index γ exceeds 2.237. To determine whether real neutron star matter is "stiff" enough to suffer from this instability we also explore here the stability of rotating neutron stars based on 13 realistic equations of state. We find that none of the 1.4 $M_\odot$ models constructed from any of these equations of state is subject to the viscous instability. In realistic equations of state, however, the overall stiffness of the model changes as the mass of the star changes. We find (in qualitative agreement with the recent results of Bonazzola, Frieben, & Gourgoulhon 1995) that very massive models constructed from four of these realistic equations of state can exhibit the viscous instability in sufficiently rapidly rotating models. In § 2 we review the formalism used here to evaluate the modes of rapidly rotating

stellar models, and in § 3 we discuss how we evaluate the secular stability of these modes due to viscous effects. In § 4 we apply these methods to evaluate the secular stability of rapidly rotating models constructed from polytropic equations of state. In § 5 we investigate the viscous instability in rapidly rotating stellar models constructed from 13 realistic neutron star equations of state.

2. THE MODES OF ROTATING STARS

In this section we describe briefly the formalism used here to evaluate the stability of the modes of rapidly rotating stellar models. Consider the perturbations of a rotating star with time dependence $e^{i\omega t}$ and angular dependence $e^{im\varphi}$, where ω is a constant, m is an integer, and φ is the angle measured about the rotation axis of the star. All of the properties of such a perturbation are determined by two scalar potentials $\delta\Phi$ and δU (Ipser & Managan 1985; Ipser & Lindblom 1989; 1990). The potential $\delta\Phi$ represents the perturbed Newtonian gravitational potential, while δU is related to the density perturbation $\delta\rho$ of the star by

$$\delta\rho = \rho \frac{d\rho}{dp} (\delta U + \delta\Phi) , \tag{1}$$

where ρ and p are the density and pressure. Quantities not preceded by δ represent their equilibrium values in the unperturbed stellar model. Here we examine only the barotropic perturbations, $\delta p = (dp/d\rho)\delta\rho$, of rigidly rotating stars. For these perturbations the velocity of the fluid in the perturbed stellar model δv^a is determined from the potential δU by

$$\delta v^a = iQ^{ab}\nabla_b \delta U . \tag{2}$$

In this equation the tensor Q^{ab} is given by

$$Q^{ab} = \frac{1}{\omega + m\Omega} z^a z^b + \frac{\omega + m\Omega}{(\omega + m\Omega)^2 - 4\Omega^2} \times \left(g^{ab} - z^a z^b - \frac{2i}{\omega + m\Omega} \nabla^a v^b \right) , \tag{3}$$

where v^a is the velocity, Ω is the angular velocity of the unperturbed star, and z^a is the unit vector parallel to the rotation axis. The Euclidean metric g_{ab} (i.e., the identity matrix in Cartesian coordinates) and its inverse g^{ab} are used to raise and lower tensor indices. The covariant derivative ∇_a associated with g_{ab} is just the partial derivative $\partial/\partial x^a$ in Cartesian coordinates. Equation (2) is equivalent to Euler's equation for these perturbations.

The two scalar potentials δU and $\delta\Phi$ are determined by the perturbed mass conservation and gravitational potential equations; these reduce to the following second-order system:

$$0 = \nabla_a(\rho Q^{ab}\nabla_b \delta U) + (\omega + m\Omega)\rho \frac{d\rho}{dp} (\delta U + \delta\Phi) , \tag{4}$$

$$0 = \nabla^a \nabla_a \delta\Phi + 4\pi G\rho \frac{d\rho}{dp} (\delta U + \delta\Phi) , \tag{5}$$

where G is Newton's gravitation constant. Equation (4) is elliptic as long as $(\omega + m\Omega)^2 > 4\Omega^2$. In this case equations (4) and (5) constitute a fairly standard elliptic eigenvalue problem that can be solved by straightforward numerical techniques once appropriate boundary conditions are imposed (Ipser & Lindblom 1990). Unfortunately, the viscosity-driven secular instability first occurs (as we discuss below) in a mode where $\omega + m\Omega = 0$. Consequently equation (4) is always hyperbolic for the cases of primary interest in this paper. Thus, the standard numerical techniques for solving elliptic eigenvalue problems fail here.

Fortunately, there exist other techniques that may be used to evaluate the eigenvalues of equations (4) and (5). In particular the Rayleigh-Ritz variational method can be applied to this problem, even in the case where equation (4) is hyperbolic. The functional,

$$S(\delta U, \omega) = \int \left\{ -\rho Q^{ab}\nabla_a \delta U^* \nabla_b \delta U + (\omega + m\Omega)\rho \frac{d\rho}{dp} \delta U^* [\delta U + \delta\Phi(\delta U)] \right\} d^3x , \tag{6}$$

is an action that is stationary with respect to infinitesimal variations in the field δU, if and only if δU satisfies equation (4) (Managan 1985; Ipser & Lindblom 1990). The functional $\delta\Phi(\delta U)$ that appears in equation (6) is defined for given δU as the solution to equation (5) with boundary condition $\delta\Phi \to 0$ as $r \to \infty$.

This action, equation (6), can be used to compute the eigenvalues of equations (4) and (5) as follows. Let δU be represented as a sum of fixed "trial" eigenfunctions δU^{jk} with real coefficients β_{jk}:

$$\delta U = \sum_{j,k} \beta_{jk} \delta U^{jk} . \tag{7}$$

Since the action $S(\delta U, \omega)$ is stationary with respect to arbitrary variations in the field δU, it must in particular be stationary with respect to variations in the coefficients β_{jk}. A necessary condition for such a δU to be a solution to equation (4) then is

$$0 = \frac{\partial S}{\partial \beta_{jk}} = 2 \sum_{j',k'} S^{jkj'k'}(\omega)\beta_{j'k'} , \tag{8}$$

where $S^{jkj'k'}(\omega)$ is defined as

$$S^{jkj'k'}(\omega) = \int \left\{ -\rho Q^{ab}\nabla_a(\delta U^{jk})^* \nabla_b \delta U^{j'k'} + (\omega + m\Omega)\rho \frac{d\rho}{dp} \times [\delta U^{j'k'} + \delta\Phi(\delta U^{j'k'})](\delta U^{jk})^* \right\} d^3x . \tag{9}$$

The system of equations (8) determines the coefficients β_{jk}. This system has a nontrivial solution if and only if

$$\det S^{jkj'k'}(\omega) = 0 . \tag{10}$$

Thus, equation (10) determines the allowed eigenvalues of the system of equations (4) and (5). Once a suitable set of trial eigenfunctions δU^{jk} are chosen, the matrix elements $S^{jkj'k'}(\omega)$ may be determined from equation (9) by (almost; see § 4) straightforward numerical integration. Then the roots of equation (10) may be evaluated (again numerically) to determine the desired eigenvalues. For the analysis of the modes of rotating stars that participate in the viscosity-driven secular instability, we find that a good choice for the trial eigenfunctions is

$$\delta U^{jk} = \left(\frac{r}{R} \right)^{|m| + 2(j+k)} Y_{|m| + 2k, m} , \tag{11}$$

where r is the spherical radial coordinate, R is the equatorial radius of the star, and Y_{lm} is the standard spherical harmonic with $l = |m| + 2k$. This choice is useful because a relatively small number of terms (as discussed below) is needed to describe the true eigenfunctions of this problem with adequate precision.

3. THE VISCOSITY-DRIVEN SECULAR INSTABILITY

The technical discussion up to this point applies (strictly speaking) only to the case of inviscid fluid stars. Our primary interest here, however, is the viscosity-driven secular instability in rotating stars. Thus, we must generalize our discussion now to include the effects of viscous dissipation on the evolution of these perturbations. Fortunately, this is not difficult to do because the effects of viscosity in realistic neutron star matter are expected to be very weak (see, e.g., Cutler & Lindblom 1987; Cutler, Lindblom, & Splinter 1990). Thus, it will be possible to include viscous effects as small corrections to the dissipation-free fluid dynamics discussed already. One convenient way to evaluate the effects of viscosity on the dynamics is to consider the functional E related to the energy of the perturbation:

$$E = \tfrac{1}{2}\int (\rho\, \delta v_a^*\, \delta v^a + \delta\rho^* \delta U) d^3x\ . \tag{12}$$

The evolution of E is easily determined using the standard theory of viscous fluid dynamics. The result is that E decreases with time in a viscous fluid according to the formula (see, e.g., Ipser & Lindblom 1991),

$$\frac{dE}{dt} = -\int 2\eta\, \delta\sigma_{ab}^*\, \delta\sigma^{ab} d^3x\ , \tag{13}$$

where η is the viscosity, and $\delta\sigma_{ab}$ is the shear of the fluid perturbation,

$$\delta\sigma_{ab} = \tfrac{1}{2}(\nabla_a \delta v_b + \nabla_b \delta v_a) - \tfrac{1}{3} g_{ab} \nabla_c\, \delta v^c\ . \tag{14}$$

The most important effect of viscosity on the modes of rotating stars is to change their frequencies from real to complex. Let $e^{i\omega t - t/\tau}$ denote the time dependence of such a mode, where ω is the real part of the frequency and $1/\tau$ is the imaginary part. The imaginary part of the frequency describes the damping (or growth) of the mode caused by the viscous dissipation. Since the functional E is real and quadratic in the perturbation quantities, its time dependence is $e^{-2t/\tau}$. Thus, the imaginary part of the frequency is related to E and its time derivative by

$$\frac{1}{\tau} = -\frac{1}{2E}\frac{dE}{dt}\ . \tag{15}$$

The functional dE/dt as defined in equation (13) is nonpositive for all fluid perturbations. Thus, the sign of the imaginary part of the frequency of a mode—and hence the stability of the mode—is determined by the sign of the energy E.

The frequency of a mode as measured in the reference frame that corotates with the star is $\omega + m\Omega$, so the stationary perturbations in this frame (if any exist) have $\omega + m\Omega = 0$. In this case the velocity perturbation δv^a vanishes, and Euler's equation (2) implies that δU is a constant. Thus, from equation (12) it follows that E vanishes for perturbations with $\omega + m\Omega = 0$ (since the integral of $\delta\rho$ vanishes for modes that do not change the total mass of the star). Thus, the vanishing of $\omega + m\Omega$ is a sufficient condition for the vanishing of the energy E. Our numerical studies show that this is also the necessary condition in the stellar models that we have investigated (although we do not know how to prove this for the general case analytically). We are interested here in studying the critical points where these instabilities first arise in certain one parameter families of rotating stellar models. As we have seen the secular stability of a mode is determined by the sign of the energy E. Thus, the points where the secular stability changes coincide with the points where the frequency $\omega + m\Omega$ vanishes. Since δv^a vanishes at these critical points, the fluid perturbations there satisfy both the viscous and the perfect fluid equations (see, e.g., Lindblom 1983). Therefore, we are able to locate a critical point where the viscous secular instability begins simply by determining where the solution to equation (10) satisfies $\omega + m\Omega = 0$.

4. POLYTROPES

We have studied the modes of rigidly rotating stellar models with polytropic equations of state. The adiabatic index γ in the polytropic equations of state,

$$p = \kappa\rho^\gamma\ , \tag{16}$$

as well as the scale factor κ are constants independent of density. (For polytropes the adiabatic index has traditionally been parameterized by the index n defined by $\gamma = 1 + 1/n$.) We constructed families of rigidly rotating polytropic stellar models (parameterized by the angular velocity $0 \le \Omega \le \Omega_{\rm Kep}$) using the numerical methods described in Ipser & Lindblom (1990). The mass, the adiabatic index γ, and the constant κ were kept fixed within any particular family of models. Figure 1 illustrates the maximum angular velocities $\Omega_{\rm Kep}$ of the stars in these families. The angular velocities in this figure are expressed in terms of the quantity $\Omega_o = (\pi G\bar{\rho}_o)^{1/2}$, where $\bar{\rho}_o$ is the average density of the nonrotating model in the family. When these maximum angular velocities are expressed in units of Ω_o,

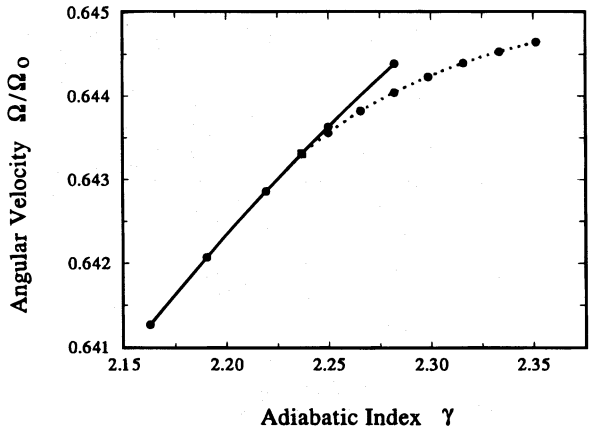

FIG. 1.—Solid curve gives the Keplerian angular velocity $\Omega_{\rm Kep}$ as a function of adiabatic index γ for rigidly rotating polytropic stellar models. Dashed curve gives the critical angular velocities, where the viscosity-driven secular instability sets in. The intersection of these curves determines the critical adiabatic index γ_c.

they depend on the adiabatic index γ but not on the mass of the star or the constant κ. The quantity $\Omega_{\rm Kep}$ is determined by computing the angular velocity of an equatorial circular orbit at the surface of each stellar model in the family and then extrapolating to find the star whose angular velocity would just match this orbital value. In order to obtain accurate values for $\Omega_{\rm Kep}$ we computed these stellar models on numerical grids containing up to 1600 radial points and 36 angular spokes. We estimate the errors of these $\Omega_{\rm Kep}$ (based on the variation of our results computed on different sized grids) to be smaller than $5 \times 10^{-7}\Omega_o$.

The frequencies of the pulsation modes for these models were determined by solving equation (10) using the trial eigenfunctions given in equation (11). The particular modes of interest to us here are the ones in which $\omega + m\Omega$ vanishes in sufficiently rapidly rotating models. These modes are referred to as $l = -m$ modes since they reduce to modes having angular dependence Y_{lm} with $l = -m$ in the nonrotating member of each family. Figure 1 illustrates the critical angular velocities, where the frequency $\omega + m\Omega$ vanishes for the $l = -m = 2$ modes. These critical angular velocities are also the points where the frequency ω of the $l = m = 2$ mode vanishes (see Ipser & Managan 1985). We have exploited this coincidence between the critical angular velocities of the $l = \pm m = 2$ modes to improve our numerical accuracy. The frequencies computed for the $l = m = 2$ modes are more accurate than those of the $l = -m = 2$ modes when a fixed number of trial eigenfunctions, equation (11), are used. The critical angular velocities that are actually displayed in Figure 1 are those of the $l = m = 2$ modes. These critical angular velocities are identical, however, to those of the $l = -m = 2$ modes because of the argument of Ipser & Managan (1985).

Figure 1 shows that the critical angular velocity of the $l = -m = 2$ mode exists only in stellar models having an adiabatic index that exceeds $\gamma_c = 2.2370 \pm 0.0008$. The corresponding critical polytropic index is $n_c = 0.8084 \pm 0.0005$. This critical value is in remarkable agreement with the original calculation of James (1964), and with a more recent relativistic analysis by Bonazzola et al. (1995). We estimate the accuracy of our calculation of the mode frequencies for individual stellar models to be less than $7 \times 10^{-7}\Omega_o$. This estimate is based on computations of the mode frequencies with various numbers of numerical grid points in the rotating star, and with various numbers of test eigenfunctions on the right side of equation (7). We use up to five angular functions, $0 \le k \le 4$, and up to 12 radial functions, $0 \le j \le 11$, in the expansion of the eigenfunction in equation (7). The critical adiabatic index is determined by finding the intersection of the $\Omega_{\rm Kep}(\gamma)$ curve with the $\Omega_c(\gamma)$ curve as displayed in Figure 1. We do this by fitting a polynomial (in the polytropic index n, see, e.g., Press et al. 1992) to the angular velocities that we compute (the large dots in Fig. 1). The intersection point that determines the critical adiabatic index is displayed as the square dot in Figure 1. The error estimate $\delta\gamma_c$ that we give for γ_c is

$$\delta\gamma_c^2 = \sum_i \left(\frac{\partial\gamma_c}{\partial\Omega_i}\,\delta\Omega_i\right)^2 , \qquad (17)$$

where the Ω_i are the individual critical and Keplerian angular velocities that we compute, and the $\delta\Omega_i$ are our estimates of the accuracy of these quantities. The partial derivatives $\partial\gamma_c/\partial\Omega_i$ are found numerically by determining how the computed γ_c varies when small changes are made in the values of the individual Ω_i.

Figure 2 illustrates more completely the angular velocity dependence of the frequencies of the $l = -m$ modes. This figure shows the frequencies of the $2 \le l = -m \le 5$ modes as computed using the techniques outlined above for the family of polytropes with $\gamma = 7/3$. We depict the angular velocity dependence of these frequencies $\omega_m(\Omega)$ in terms of the dimensionless function $\alpha_m(\Omega)$ defined by

$$\alpha_m(\Omega) = \frac{\omega_m(\Omega) + m\Omega}{\omega_m(0)} . \qquad (18)$$

This function is scaled so that its value is unity, $\alpha_m(0) = 1$, for nonrotating stars and vanishes whenever the secular instability of one of these modes changes. This figure illustrates that the $l = -m = 2$ mode is the only one where $\omega + m\Omega$ changes sign. Thus, it is only the $l = -m = 2$ mode that is subject to the viscous instability in these stars. These curves confirm our expectation, based previously only on our understanding of the corresponding modes of the Maclaurin spheroids (see, e.g., Lindblom 1987), that the higher order $l = -m$ modes can be unstable only if the $l = -m = 2$ mode is unstable.

The dashed portion of the $m = -2$ curve in Figure 2 represents interpolated rather than directly computed frequencies. And, the other curves in Figure 2 do not extend all the way to the Keplerian angular velocity. In these regions our numerical methods appear to fail. In general the eigenfunctions that we compute have the strictly monotonic (in r) behavior of f-modes. For certain ranges of angular velocity (in particular the dashed portion of this $m = -2$ curve), however, the eigenfunctions of the $l = -m$ modes develop maxima and even nodes in some cases. When this occurs the accuracy of the solution is reduced (for a fixed number of trial eigenfunctions), and in extreme cases the computed frequencies no longer follow smooth curves as depicted in Figure 2. We do not fully understand the reason our numerical method fails in these regions. It is possible that the trial eigenfunctions, equation (11), that we use are poor representations of the real eigenfunctions in these regions. It is also possible that some real physical process—like a degeneracy between the f and p_1 modes—makes our

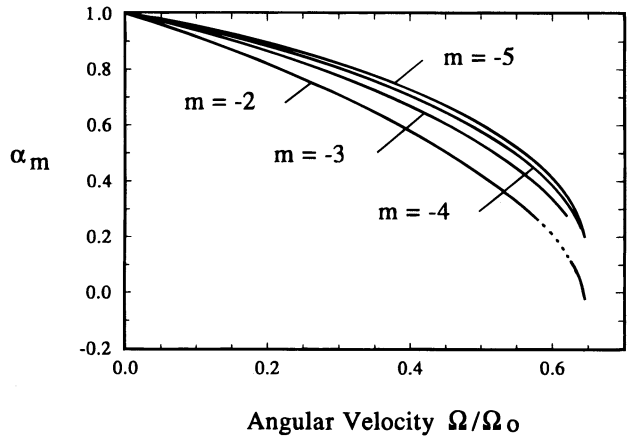

FIG. 2.—Angular velocity dependences of the frequencies of the $l = -m$ modes of rigidly rotating $\gamma = 7/3$ polytropes. The function α_m is defined as $\alpha_m(\Omega) = [\omega_m(\Omega) + m\Omega]/\omega_m(0)$.

numerical algorithm singular. This problem, whatever its origin, does not affect in any way the results presented in Figure 1.

We need to discuss one technical detail associated with the numerical techniques used here to evaluate the frequencies of the modes of these rotating polytropes. The integral that appears on the right side of equation (9) contains the factor $\rho\, d\rho/dp$. This quantity diverges at the surface of any polytropic stellar model with $\gamma \geq 2$. While these integrals are finite, the standard numerical integration techniques do not converge rapidly in this case. Therefore, we have developed a somewhat nonstandard numerical method to obtain faster convergence, and for completeness we describe it briefly here. In a polytrope the function $\rho\, d\rho/dp$ equals $K(R-r)^{(2-\gamma)/(\gamma-1)}$ plus higher order terms in $R-r$, where r is the radial coordinate, $R(\theta)$ is the radius of the star in a given angular direction, and $K(\theta)$ is independent of r. Thus, the integrands that appear in equation (9) are all of the form $f(r,\theta)(R-r)^{(2-\gamma)/(\gamma-1)}$, where f is a smooth and bounded function. We perform the radial integrals of these functions using low-order methods such as the trapezoidal rule, while the angular integrals are performed with Gaussian quadrature. If r_N represents the last radial grid point within the star, $r_N < R < r_{N+1}$, then the radial integral of the singular portion of this integrand would be approximated as

$$\int_{r_{N-1}}^{R} f(r,\theta)(R-r)^{(2-\gamma)/(\gamma-1)}\,dr \approx \frac{\Delta r}{2} f(r_{N-1},\theta)(R-r_{N-1})^{(2-\gamma)/(\gamma-1)} + \Delta r f(r_N,\theta)(R-r_N)^{(2-\gamma)/(\gamma-1)}, \quad (19)$$

where $\Delta r = r_N - r_{N-1}$. Unfortunately, this approximation completely misses the singular portion of the integrand between the last grid point r_N and the surface of the star R. Since we know the structure of this singular behavior, however, we can perform the singular portion of the integral analytically and use this information to construct a more accurate algorithm. The integral of $(R-r)^{(2-\gamma)/(\gamma-1)}$ between r_N and R gives $(\gamma-1)(R-r_N)^{1/(\gamma-1)}$. Thus, using the trapezoidal rule to integrate between r_{N-1} and r_N, and adding the lowest order contribution from the singular portion of the integrand between r_N and R, we arrive at the following improved numerical algorithm for the radial integral of the singular part of the integrand:

$$\int_{r_{N-1}}^{R} f(r,\theta)(R-r)^{(2-\gamma)/(\gamma-1)}dr \approx \frac{\Delta r}{2} f(r_{N-1},\theta)(R-r_{N-1})^{(2-\gamma)/(\gamma-1)} + \Delta r C(\theta) f(r_N,\theta)(R-r_N)^{(2-\gamma)/(\gamma-1)}, \quad (20)$$

where $C(\theta)$ is defined as

$$C(\theta) = \frac{1}{2} + (\gamma-1)\frac{R-r_N}{\Delta r}. \quad (21)$$

Comparing equation (20) with equation (19) we see that the only change is to replace the function $f(r_N,\theta)$ with the quantity $C(\theta)f(r_N,\theta)$ for the last grid points within the star. We have used this technique to evaluate all of the integrals involved in determining the matrix elements $S^{jkj'k'}$. We note that the second term in equation (5) also has this type of singular behavior. Therefore, when the functional $\delta\Phi(\delta U)$ is evaluated numerically to determine $\delta\Phi$ for a given δU, the same numerical difficulty arises. Fortunately, this problem can be corrected in precisely the same way. We modify the matrix elements that represent the differential operator and those representing the δU source by multiplying the terms containing $\rho\, d\rho/dp$ on the last grid points within the star by the factor $C(\theta)$ as explained above. This simple modification significantly improves the numerical convergence of these integrals.

5. REALISTIC EQUATIONS OF STATE

Until now our understanding of the viscosity-driven secular instability has been limited to stellar models based on the idealized polytropic equations of state discussed in the previous section. The numerical techniques that we use here do not depend in any essential way on the details of the equation of state, however. Therefore, it is a relatively straightforward exercise to use these techniques to test for secular instabilities in stellar models based on more realistic equations of state. We have carried out this analysis for neutron star models based on a set of 13 realistic equations of state. Twelve of these (which we refer to by the abbreviations BJI, DiazII, FP, Glend1, Glend2, Glend3, HKP, PandN, WFF1, WFF2, WFF3, and WGW) are described in some detail by Salgado et al. (1994). We add to this list one additional equation of state (referred to here as SHW), which is based on the relativistic-mean-field calculation of Serot (1979) as described in Lindblom & Mendell (1994). Figure 3 illustrates the angular velocity dependence of the $l=-m=2$ modes in the 1.4 $M_\odot$ stellar models constructed from each of these equations of state. These curves illustrate that the angular dependence of the frequencies of these modes is extremely insensitive to the equation of state. We truncate each of the curves in Figure 3 at the angular velocity where the computed eigenfunction develops a

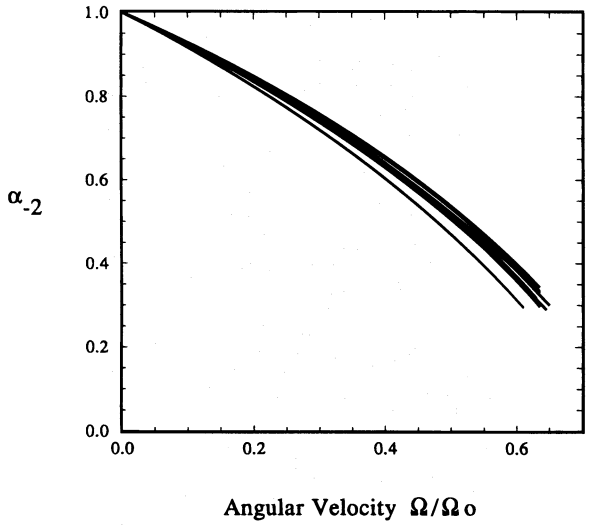

FIG. 3.—Angular velocity dependences of the $l=-m=2$ modes in the rigidly rotating 1.4 $M_\odot$ stellar models constructed from 13 realistic equations of state.

maximum, signaling the onset of the numerical difficulty described in § 4. These numerical difficulties occur only for large angular velocities in these models ($\Omega \gtrsim 0.88\Omega_{\rm Kep}$), and the (possibly unreliable) frequencies computed beyond this point show no sign of deviating from smooth extrapolations of the displayed portions of these curves. Thus, Figure 3 illustrates that none of these realistic 1.4 $M_\odot$ neutron star models is subject to a secular instability in the $l = -m = 2$ mode since $\omega - 2\Omega$ is strictly positive in each of these models. Figure 4 illustrates the angular velocity dependence of the $2 \leq l = -m \leq 5$ modes in the 2.994 $M_\odot$ stellar models (the maximum nonrotating general relativistic mass) based on the SHW equation of state. This figure demonstrates, as in the polytropic case, that the higher $l = -m$ modes are stable if the $l = -m = 2$ mode is. Thus, we find no evidence for a viscosity-driven secular instability in 1.4 $M_\odot$ neutron stars. The dashed portion of the $m = -2$ curve and the (missing) highest angular velocity sections of the $m = -3$ and -4 curves in Figure 4 represent, as in Figure 2, regions where our numerical method fails to find modes with monotonic (in r) eigenfunctions.

The adiabatic index γ is a function of the density in the realistic equations of state. Stars with different masses contain different proportions of material with different adiabatic indices. Thus, the overall stiffness of the stellar model, and hence its susceptibility to the viscosity-driven secular instability, depends on its mass. We have examined the stability of the rotating stellar models based on the 13 realistic equations of state described above for a wide range of neutron star masses. In nine of these (BJI, DiazII, FP, Glend1, Glend2, Glend3, PandN, WFF2, WFF3) we find no secular instability points at all over a very wide range of masses. In the analysis here we use the Newtonian equations to determine the equilibrium structures and the dynamical evolution of the modes. These Newtonian equations allow much larger mass equilibrium solutions than their general relativistic counterparts. A number of general relativistic effects contribute to this difference: (1) in general relativity the pressure acts as a source of the gravitational field and makes the gravitational attraction stronger than it would be in Newtonian theory, and (2) the (negative) gravitational binding energy of the system lowers the gravitational mass of the general relativistic configuration compared to its Newtonian counterpart. In an attempt to include the full range of Newtonian models with general relativistic counterparts, we tested the stability of these models with masses up to twice the maximum mass for rigidly rotating fully relativistic configurations (see Bonazzola et al. 1995). In four equations of state (HKP, SHW, WFF1, WGW) we do find secular instabilities in sufficiently massive models. Table 1 summarizes the minimum mass where this instability is first seen in models having these equations of state. We also list in Table 1 the rotation periods of these stars where the instability first sets in. In the SHW equation of state this minimum mass is slightly less than the maximum mass allowed for nonrotating general relativistic configurations. In the other three equations of state the minimum mass for instability exceeds even the maximum rotating general relativistic mass.

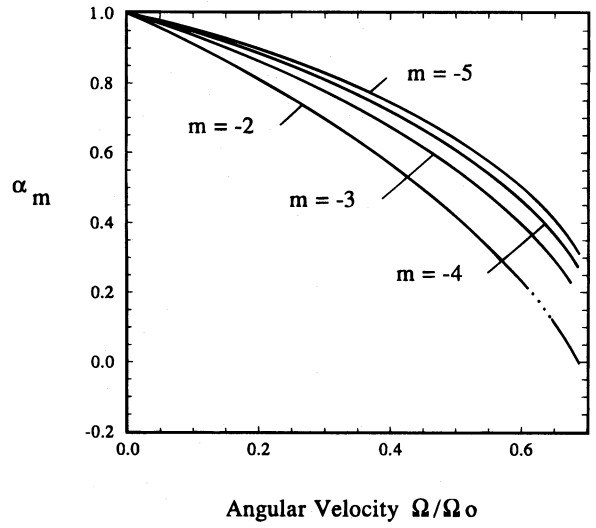

FIG. 4.—Angular velocity dependences of the $l = -m$ modes in the rigidly rotating $M = M_{\rm max}$ stellar models constructed from the SHW equation of state.

TABLE 1

CRITICAL MASSES FOR THE VISCOUS INSTABILITY

Equation of State	$M_{\rm max}/M_\odot$ [a]	$M_{\rm crit}/M_\odot$ [b]	$M_{\rm crit}/M_{\rm max}$	$P_{\rm crit}$ [c] (ms)
SHW	2.994	2.91	0.97	1.188
HKP	2.827	5.04	1.78	1.180
WFF1	2.123	4.91	2.31	0.760
WGW	1.967	4.16	2.11	1.062

[a] $M_{\rm max}$ is the maximum mass of a nonrotating general relativistic stellar model. The values of $M_{\rm max}$ for HKP, WFF1, and WGW are from Bonazzola et al. 1995.

[b] $M_{\rm crit}$ ($\pm 0.02\ M_\odot$) is the minimum mass for which the viscous secular instability is found in sufficiently rapidly rotating models.

[c] $P_{\rm crit}$ (± 0.002 ms) is the rotation period where the viscous secular instability sets in for stars with $M = M_{\rm crit}$.

Recently, Bonazzola et al. (1995) have also investigated the secular instability of rotating stars using a rather different type of analysis. They use a fully relativistic numerical code to determine the equilibrium structures of the rotating stars, and analyze the dynamics of the fluid to test for stability using an approximation to the full relativistic hydrodynamic equations. They find secular instabilities in stars based on the FP, HKP, WFF1, WFF2, and WFF3 equations of state in sufficiently massive stars. Their results are, therefore, in qualitative agreement with ours: we both find the viscosity-driven secular instability in the very massive models of selected equations of state. Since they find instabilities in stars having lower masses and in more equations of state than in the Newtonian analysis presented here, it suggests that relativistic effects tend to enhance the viscosity-driven secular instability in these models. This is consistent with the post-Newtonian enhancement of the gravitational radiation-driven secular instability found by Cutler & Lindblom (1992). Unfortunately, even with this enhancement these results reveal that the viscosity-driven secular instability only occurs in very massive neutron stars: stars with masses considerably larger than the 1.4 $M_\odot$ binary radio pulsars, which are presently the only accurately measured neutron star masses.

We thank Eric Gourgoulhon for helpful comments and for supplying us with most of the realistic neutron star equation of state tables used in § 4. This research was supported in part by grant PHY-9019753 from the National Science Foundation.

REFERENCES

Bonazzola, S., Frieben, J., & Gourgoulhon, E. 1995, ApJ, 459, in press
Chandrasekhar, S. 1970, Phys. Rev. Lett., 24, 611
Cook, G. B., Shapiro, S. L., & Teukolsky, S. A. 1994, ApJ, 424, 823
Cutler, C., & Lindblom, L. 1987, ApJ, 314, 234
———. 1992, ApJ, 385, 630
Cutler, C., Lindblom, L., & Splinter, R. J. 1990, ApJ, 363, 603
Friedman, J. L. 1978, Comm. Math. Phys., 62, 247
Friedman, J. L., Ipser, J. R., & Parker, L. 1989, Phys. Rev. Lett., 62, 3015
Friedman, J. L., & Schutz, B. F. 1977, ApJ, 222, 281
Haensel, P., Salgado, M., & Bonazzola, S. 1995, A&A, 296, 745
Ipser, J. R., & Lindblom, L. 1989, Phys. Rev. Lett., 62, 2777
———. 1990, ApJ, 355, 226
———. 1991, ApJ, 373, 213
Ipser, J. R., & Managan, R. A. 1985, ApJ, 292, 517
James, R. A. 1964, ApJ, 140, 552
Lattimer, J. M., Prakash, M., Masak, D., & Yahil, A. 1990, ApJ, 355, 241
Lindblom, L. 1983, ApJ, 267, 402
Lindblom, L. 1987, ApJ, 317, 325
———. 1995, ApJ, 438, 265
Lindblom, L., & Detweiler, S. L. 1977, ApJ, 211, 565
Lindblom, L., & Hiscock, W. A. 1983, ApJ, 267, 384
Lindblom, L., & Mendell, G. 1994, ApJ, 421, 689
———. 1995, ApJ, 444, 805
Managan, R. A. 1985, ApJ, 294, 463
Press, W. H., Teukolsky, S. A., Vetterling, W. T., Flannery, B. P. 1992, Numerical Recipes in FORTRAN: The Art of Scientific Computing (2d ed.; Cambridge: Cambridge Univ. Press)
Roberts, P. H., & Stewartson, K. 1963, ApJ, 137, 777
Salgado, M., Bonazzola, S., Gourgoulhon, E., & Haensel, P. 1994, A&A, 291, 155
Serot, B. D. 1979, Phys. Lett. B, 86, 146
Thompson, W., & Tait, P. G. 1883, Principles of Natural Philosophy (Oxford: Clarendon)